CrossMark

REGULAR ARTICLE

Mechanism of *Lycium barbarum* polysaccharides on primary cultured rat hippocampal neurons

Peng Zhao[1] · Ning-Tian Ma[1] · Ren-Yuan Chang[2] · Yu-Xiang Li[3] · Yin-Ju Hao[1] ·
Wen-Li Yang[1] · Jie Zheng[1] · Yang Niu[4] · Tao Sun[5] · Jian-Qiang Yu[1,6]

Abstract *Lycium barbarum* polysaccharides (LBP) have been reported to have a wide range of beneficial effects including neuroprotection, anti-aging and anticancer. However, the anti-inflammation mechanism of LBP on primary cultured rat hippocampal neurons injured by oxygen-glucose deprivation/reperfusion (OGD/RP) is incompletely understood. We investigate the neuroprotective effects of LBP on neonatal rat primary cultured hippocampal neurons injured by OGD/RP with different approaches: MTT assay was used to detect cell viability, lactate dehydrogenase leakage was used to detect neuronal damage, formation of reactive oxygen species was determined by using fluorescent probe DCFH-DA. Hoechst 33,342 staining and TUNEL staining were used to determine the cell apoptosis. JC-1 was used to evaluate loss of mitochondrial membrane potential (MMP). The fluorescence intensity of $[Ca^{2+}]_i$ in hippocampal neurons was determined by laser scanning confocal microscopy. The expression of various apoptotic markers such as TLR4, IκB, IL-6 and NF-κB were investigated by RT-PCR and western blot analysis. Results from each approach demonstrated that LBP increased the cell abilities and decreased the cell morphologic impairment. Furthermore, LBP increased MMP but inhibited $[Ca^{2+}]_i$ elevation and significantly suppressed overexpression of NF-κB, IL-6 TLR4 and increased IκB expression.

Peng Zhao and Ning-Tian Ma Contributed equally to this study.

✉ Jian-Qiang Yu
yujq910315@163.com

[1] Department of Pharmacology, Ningxia Medical University, 1160 Shengli Street, Yinchuan 750004, Ningxia, People's Republic of China

[2] Pharmacy Department of Yulin First Hospital, Shaanxi 719000, China

[3] College of Nursing, Ningxia Medical University, Yinchuan 750004, China

[4] Key Laboratory of Hui Ethnic Medicine Modernization, Ministry of Education, Ningxia Medical University, Yinchuan 750004, China

[5] Key Laboratory of Craniocerebral Diseases of Ningxia Hui Autonomous Region, Ningxia Medical University, Yinchuan 750004, China

[6] Ningxia Hui Medicine Modern Engineering Research Center and Collaborative Innovation Center, Ningxia Medical University, Yinchuan 750004, China

Introduction

Brain ischemia is the fourth commonest cause of death and the leading cause of long-term disability in industrialized countries (Burke et al. 2012). In China, there are 58–142 per 100,000 people each year who die of stroke (Zhao and Liu 2016). And the number of global deaths caused by stroke is projected to rise to 6.5 million in 2015 and to 7.8 million in 2030 (Strong et al. 2007). Accordingly, there is much interest in therapeutic intervention to decrease neurological damage and prevent death after stroke. New treatment options are critically needed to extend the therapeutic window for Chinese medicinal herbs and provide neuroprotection to slow cell death after stroke.

Wolfberry, the fruit of *L. barbarum*, is produced mainly in Ningxia, China and *L. barbarum* has been used as a food additive as well as a medicinal herb in many Asian countries for more than 1000 years (Zhang et al. 2005; Chang and So 2008). It plays an important role in preventing and treating various chronic diseases. *Lycium barbarum* polysaccharides

(LBP) can modulate the immune function (Huyan et al. 2014; Zhao et al. 2014), act against the effects of aging and oxidation (Zhou et al. 2016a, b; He et al. 2014), protect against liver damage (Varoni et al. 2016), promote retinal progenitor cell proliferation (Wang et al. 2015a, b), exert anti-cancer effects (Zhang et al. 2016) and protect neurons in an animal model of oxygen-glucose deprivation/reperfusion (OGD/RP) by inhibiting neuronal apoptosis (Wang et al. 2014; Rui et al. 2012).

Accumulating evidence shows that TLRs (Toll-like receptors) are activated by endogenous proteins released from damaged brain and play a crucial role in mediating the cerebral injury following ischemia and reperfusion (Kaczorowski et al. 2008). In particular, TLR2 and TLR4 have been found to be more important than other TLRs in the pathologic progression of cerebral ischemia and reperfusion (Krmpotić et al. 2013). Therefore, TLRs have become a potential target in searching for a new strategy for the treatment of ischemic cerebrovascular disease. TLR4 signals activate downstream effectors that include NF-κB, mitogen-activated protein kinase (MAPK) and phosphatidylinositol 3-kinase (PI3K), through adaptor proteins including MyD88. Collectively, these pathways regulate the expression of pro-inflammatory cytokines and genes that control cell survival and apoptosis.

Although some scholars have demonstrated that co-administration with LBP evidently attenuates hepatic steatosis, fibrosis, oxidative stress, inflammation and apoptosis in rats and neurons (Xiao et al. 2014), we still do not know whether LBP could play a therapeutic role against the development of inflammatory response, which is connected with TLR4/NF-κB activation. In the current study, we mainly focus on the therapeutic effects and mechanisms of LBP on an already established OGD/RP model.

Material and methods

Experiment animals

Adult male and female Sprague–Dawley rats (150-200 g) and newborn Sprague–Dawley rats (less than 24 h old) were obtained from the Experimental Animal Center of Ningxia Medical University (Ningxia, China). They were maintained in accordance with internationally accepted principles for laboratory animal use. All experimental protocols were approved by the Committee for Laboratory Animal Management of Ningxia Medical University (Chinese License Key Number: SCXK Ningxia: 20,050,001). They conformed to the National Institutes of Health guidelines on the ethical use of animals. This study was approved by the Local Ethics Committee in March 2009.

Reagents

LBP was supplied by Qinghai General Health Bio-science, Qinghai, China (Lot No.: KPGQZTQW-13-02, purity > 60%). Nimodipine injection (Nim) (PubChem CID: 4497) was obtained from Bayer, Germany (Lot No.: BXFS1Kb, 0.2 mg/ml). The reagents used in this experiment are as follows: Dulbecco's Modified Eagles Medium (DMEM; Gibco), Neurobasal-A-Medium (Gibco), fetal bovine serum (Gibco), B-27 Supplement (Gibco), 0.25% Trypsin (Gibco), Poly-L-Lysine (PLL; Gibco), HEPES buffered saltsolution (Gibco), Earle's balanced salt solution (EBSS) (in mg/L: 6800 NaCl, 400 KCl, 264 $CaCl_2 \times H_2O$, 200 $MgCl_2 \times 7 H_2O$, 2200 $NaHCO_3$, 140 $NaH_2PO_4 \times H_2O$, and 1000 glucose, pH 7.2), phosphate buffered saline (PBS), 3-(4,5-dimethyl thiazol-2-yl)-2,5-diphenyltetrazolium bromide (MTT; Solarbio). The commercial kit for the detection of mitochondrial membrane potential (MMP), calcium fluorescence probe (Fluo-3 AM) and Hoechst 33342 were purchased from Beyotime Institute of Biotechnology (Jiangsu Province, China). The commercial kits for the detection of lactate dehydrogenase (LDH) and reactive oxygen species (ROS) were obtained from Nanjing Jiancheng Bioengineering Institute (Nanjing, China). TUNEL staining was performed by In Situ Cell Death Detection Kit (Roche, Germany). AxyPrep Multisource Total RNA Miniprep Kit was obtained from Axygen Scientfic. Other commercial kits, Transcript RT/RI Enzyme Mix and TransStart Top Green qPCR SuperMix, were purchased from TransGen Biotech (Beijing, China). Antibody of TLR4 was purchased from Wuxin AppTec (San Diego, USA). Antibody of β-actin, IκB-α, IL-6 and NF-κB were purchased from Proteintech (Chicago, USA). All other reagents were from commercial sources and of standard biochemical quality.

Hippocampal neuron culture and OGD/RP

Primary hippocampal neuronal cells were prepared from newborn Sprague–Dawley rats. After trituration and trypsinization, viability of hippocampal neurons was above 95% as calculated using conventional trypan blue staining, under an optical microscope. Single-cell suspensions were plated at a density of 1×10^6/ml, seeded in PLL-coated 6-well or 96-well plates and were cultured in DMEM supplemented with 10% fetal bovine serum and 2% HEPES buffered salt solution. Cells were maintained in a humidified incubator (37 °C with 5% CO_2) for 1.5 h to achieve well-adherent cells. DMEM culture medium was removed and replaced with 2% B-27 of Neurobasal-A-Medium culture medium. After that, half of the culture medium was replaced with fresh culture medium every 2 days (Rui et al. 2012). In preliminary experiments in our laboratory, hippocampal neuron fluorescence staining with rabbit anti-rat neuron specific

enolase (NSE) had been performed to identify the neurons as described by Zhao et al. (2012).

Neurons were washed with EBSS without glucose for three times and then the culture media were replaced with glucose-free EBSS incubated for 2 h in oxygen-free $N_2/CO_2(95\%/5\%)$ gas at 37 °C. Then, the cultures were incubated again in a normoxic incubator with normal culture medium for an additional 24 h as reperfusion. The cultures of the control group were not exposed to OGD/RP. Other treating processes were as same as the injury groups. Cells were randomly divided into 6 groups: control group; vehicle (OGD/RP) group; Nim group (5 mg/l); low, middle and high concentration LBP (10, 20 and 40 mg/l) groups. LBP was given at the start of the reperfusion phase, acting through the processes of reperfusion.

MTT and LDH assay

Cell viability was assessed by the measurement of formazan. MTT was added to 96-well plates after the above cell treatment protocol at a final concentration of 5 mg/ml. After 4 h incubation, formazan formed, the medium was removed and cells were dissolved in DMSO. The formation of formazan was measured by spectrophotometry at 490 nm using an ELISA reader (ELx800uv; Bio Tek Instruments, USA). Neuronal damage was also quantitatively assessed by measuring the activity of LDH, released from damaged or dead cells. A previous study showed that the efflux of LDH occurring from either necrotic or apoptotic cells is proportional to the number of neurons damaged or destroyed (Gwag et al. 1995). LDH activity in the medium and total activity was measured by LDH assay kit at 440 nm. The percentage of LDH leakage was expressed as (LDH activity in medium/total activity) × 100%.

Measurement of reactive oxygen species (ROS)

Formation of ROS was determined by using fluorescent probe DCFH-DA. Cell-permeant nonfluorescent DCFH-DA has been shown to be oxidized to high-fluorescent 2,7-dichlorofluorescin in the presence of ROS. Neurons were washed twice with phosphate-buffered saline (PBS) and then incubated with DCFH-DA (10 mM) for 30 min at 37 °C in the dark. The cells were harvested and suspended in PBS. The fluorescence intensity was measured by fluorospectro photometer at an excitation wavelength of 485 nm and an emission wavelength of 525 nm.

Hoechst 33342 staining and TUNEL staining

To detect the characteristic features of apoptotic nuclei, the cultured hippocampal neurons were stained with 10 μM Hoechst 33342. Briefly, cells were washed with PBS twice and fixed for 20 min in 4% (w/v) paraformaldehyde at room temperature. After 30 min, the cells were rinsed three times with PBS to remove the 4% (w/v) paraformaldehyde and then exposed to 10 μM Hoechst 33342 for 5 min at 37 °C in the dark. The dye was removed by washing three times with PBS. The stained nuclei were visualized and analyzed by laser scanning confocal microscopy (Tokyo, Japan). We counted cell numbers and measured the apoptotic rate.

Briefly, cells were plated at a density of $1 × 106$/ml, seeded in PLL-coated 6-well plates. Twenty-four hours after reperfusion, cells were fixed by immersing slides in 4% methanol-free formaldehyde solution for 20 min at room temperature and permeabilized with 0.2% Triton X-100 for 5 min. Cells were labeled with fluoresce in TUNEL reagent mixture for 60 min at 37 °C according to the manufacturer's suggested protocol. After that, slides were examined by fluorescence microscopy (Nikon, Tokyo, Japan) and the number of TUNEL-positive (apoptotic) cells was counted.

Measurement of $[Ca^{2+}]_i$ of hippocampal neuronal cells

The primary hippocampal neurons were cultured in Petri dishes with a coverslip. Cells were washed with Hank's solution twice and then loaded with 10 μmol/l Fluo-3/AM for 30 min at 37 °C in the dark. After 30 min at 37 °C, the cells were rinsed three times with Hank's solution to remove the extracellular Fluo-3/AM. The fluorescence intensity of $[Ca^{2+}]_i$ in hippocampal neurons was determined by laser scanning confocal microscopy. Total images were scanned and the data were stored in disks for analysis (Rui et al. 2012).

Determination of mitochondrial membrane potential (MMP)

We measured MMP by mitochondrial membrane potential assay kit with JC-1, using the confocal laser scanning microscope. JC-1 is a convenient voltage sensitive probe to monitor MMP (Reers et al. 1991). Cells containing forming J-aggregates have high $\triangle\Psi m$ and show red fluorescence. Cells with low $\triangle\Psi m$ are those in which JC-1 maintains (or reacquires) monomeric form and show green fluorescence (Zhu et al. 2009). The relative proportions of red and green fluorescence were used to measure the ratio of mitochondrial depolarization.

Reverse transcription real-time quantitative PCR assay

Expressions of NF-κB, IL-6, IκB-α and TLR4 mRNA were detected using real-time quantitative PCR. Total RNA of primary cultured neurons was isolated by Trizol agent. Denaturing agarose gel electrophoresis was used for the detection of the concentration and purity of RNA. RNA was reverse-transcribed with TransScript First-Strand cDNA Synthesis SuperMix. The nucleotide sequences of the primers

used in this study were as follows: 5′-GTG TTC ACA GAC CTG GCA TC-3′ (forward) and 5′-TTC AGG GTA CTC CAT CAG CA-3′ (reverse) for NF-κB; 5′-TTA CGA GCA GAT GGT GAA GG-3′ (forward) and 5′-TTC ATG GAT GAT TGC CAA GT-3′ (reverse) for IκB-α; 5′-ACT TCA CAA GTC GGA GGC TT-3′ (forward) and 5′-AGT GCA TCA TCG CTG TTC AT-3′ (reverse) for IL-6; 5′-GAT TGC TCA GAC ATG GCA GT-3′ (forward) and 5′-CCC ACT CGA GGT AGG TGT TT-3′ (reverse) for TLR4; 5′-CCC ATC TAT GAG GGT TAC GC-3′ (forward) and 5′-TTT AAT GTC ACG CAC GAT TTC-3′ (reverse) for β-actin. The TransStart Top Green qPCR SuperMix kit was used for real-time quantitative PCR analysis (initial template denaturation at 94 °C for 5 min, followed by 35 cycles of 94 °C for 30 s, 61 °C for 30 s and 72 °C for 1 min). The relative changes in expression of the amplified gene was determined using a comparative cycle threshold (Ct) method with $2^{-\Delta\Delta Ct}$ (Livak and Schmittgen 2001).

Western blot analysis

To determine the levels of NF-κB, IL-6, IκB-α and TLR4 protein expression, the primary hippocampal neurons were subjected to western blot analysis. The protein was extracted using lysis buffer containing protease inhibitor, phosphatase inhibitor and 100 mM phenylmethylsulfonyl fluoride (PMSF) (KeyGEN, Nanjing, China). The supernatant was obtained by centrifugation at $12{,}000g$ for 15 min at 4 °C. The protein content was assayed by BCA protein assay (KeyGEN). Aliquots of 30 mg of protein were treated with Laemmli sample buffer (GenDEPOT, USA), heated at 100 °C for 5 min and electrophoresed with 25 mg/lane in a 10% acrylamide denaturing SDS-polyacrylamide gel (SDS–PAGE). After transferring to PVDF membranes, the membrane was then incubated in blocking buffer (1 × PBS, 0.1% Tween 20 and 5% non-fat milk) for 1 h at room temperature, followed by overnight incubation at 4 °C with primary antibodies of NF-κB, IL-6, IκB-α, TLR4 and β-actin. Primary antibodies

for NF-κB (65 kDa, rabbit polyclonal antibody, 1: 2500 dilution; Proteintech), IL-6 (30 kDa, rabbit monoclonal antibody, 1:1000 dilution; Proteintech), IκB-α (36–40 kDa, rabbit monoclonal antibody, 1:200–1:2000 dilution; Proteintech), TLR4 (95 kDa, rabbit monoclonal antibody, 1:1000 dilution; Wuxi AppTec), β-actin (42 kDa, rabbit polyclonal antibody, 1:4000 dilution; Proteintech) were used. β-actin served as an internal control. The peroxidase-conjugated affinipure goat anti-rabbit IgG (1:7000; ZSGB-Bio) secondary antibody was incubated for 1 h at room temperature and detected with a chemiluminescent agent (ECL; Amersham Life Sciences). Band densities were measured using Quantity One 1-D Analysis software v.4.6.9 (Bio-Rad Laboratories, USA) and were used for analysis.

Statistical analysis

All quantitative data were expressed as mean ± SD. The significance of differences in means between control and treated groups for different parameters was determined by one-way analysis of variance (ANOVA). The significance of differences between vehicle and control group was evaluated by Student's t test. The software package SPSS 18.0 was used for calculations. P values of less than 0.05 were considered statistically significant.

Results

MTT and LDH assay

As shown in Fig. 1 an exposure to OGD resulted in decreased cell viability compared to the control group as assessed using the MTT assay. Cell viability was 98.72 ± 0.2% in the control group, 28.68 ± 0.3% in the OGD/RP group, 49.53 ± 0.14% in the OGD group treated with 10 mg/l LBP, 57.16 ± 0.58% in the OGD group treated with 20 mg/l LBP and 66.72 ± 0.24% in the OGD group treated with 40 mg/l LBP. Thus, cells
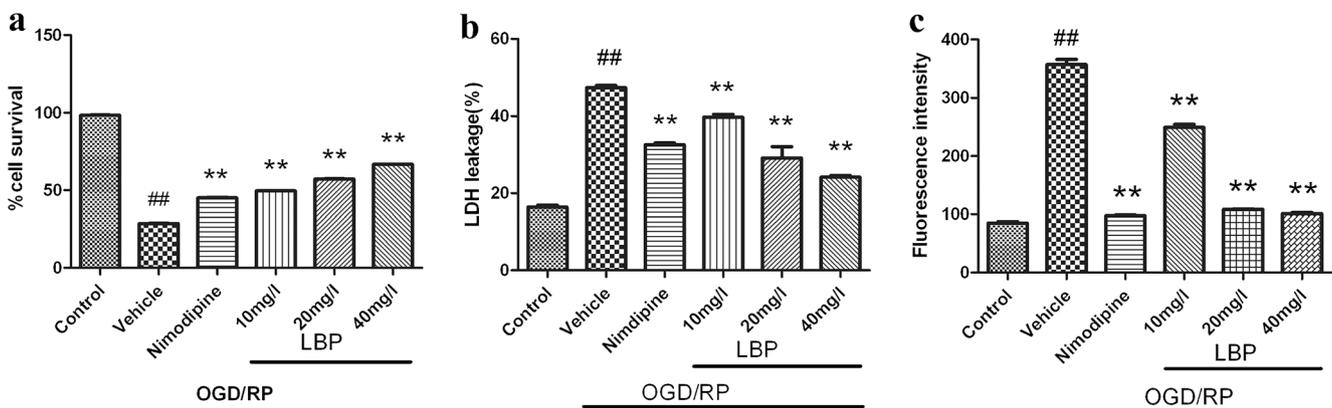

Fig. 1 Effects of LBP on cell viability in primary hippocampal neuronal cells under OGD 2 h/RP 24 h, determined by MTT assay (**a**), the extent of LDH release (**b**) and ROS. Data represent mean ± SD, $n = 6$. $^{##}p < 0.01$ Vehicle group vs. Control group; $^{*}p < 0.05$, $^{**}p < 0.01$ vs. Vehicle group

treated with LBP prior to the OGD/RP group were significantly more viable than cells not pre-treated with LBP. Treatment of neuronal cells with LBP followed by OGD exposure resulted in dose-dependent protection. In particular, the increase in cell viability in the OGD/RP group treated with 40 mg/l LBP was significantly greater than that of the untreated OGD/RP group ($P < 0.01$).

LDH leakage corresponds to cytotoxicity and membrane damage. The percentage cytotoxicity based on LDH measurements was $47.4 \pm 0.95\%$ in the OGD/RP group ($P < 0.01$ compared with control group), $39.7 \pm 1.3\%$ in the OGD/RP group treated with 10 mg/l LBP, $32.37 \pm 0.67\%$ in the OGD/RP group treated with 20 mg/l LBP and $24.3 \pm 1.2\%$ in the OGD group treated with 40 mg/l LBP (Fig. 1b). There was a significant decrease in LDH leakage in all OGD/RP groups treated with LBP compared to the vehicle group ($P < 0.01$).

Measurement of ROS

Intracellular ROS levels were monitored using the fluorescent dye DCFH-DA. Figure 1c shows the accumulation of ROS in neuronal cells exposed to OGD/RP. Treatment with LBP inhibited ROS accumulation in neuronal cells after OGD/RP. A significant decrease in ROS formation was found in the OGD/RP groups treated with LBP compared to the vehicle group ($P < 0.05$). ROS levels were 85 ± 5 in the control group and 356.6 ± 15.14 in the OGD/RP group that did not receive LBP treatment, while the ROS level was 101 ± 3.6 in the OGD/RP group treated with 40 mg/l LBP, 110 ± 4.3 in the OGD group treated with 20 mg/l LBP and 247.67 ± 10.78 in the OGD group treated with 10 mg/l LBP.

Measurement of $[Ca^{2+}]_i$

We further investigated whether the $[Ca^{2+}]_i$ was affected (Fig. 2). OGD/RP insults resulted in a rapid increase in intracellular Ca^{2+}. At the end of an OGD/RP insult, a significant elevation of $[Ca^{2+}]_i$, which was nearly 3.5-fold of that under normal conditions, was observed in the insulted neurons. Nim, a Ca^{2+} blocker used to relax the cerebral vasculature, could to some extent depress the elevation of $[Ca^{2+}]_i$ in OGD/RP-insulted cells. Similarly, LBP also obviously inhibited the elevation of $[Ca^{2+}]_i$ induced by OGD/RP in a concentration-dependent manner. Consistent with the findings of the apoptosis experiment, the inhibitory effect of 40 mg/l LBP on the elevation of $[Ca^{2+}]_i$ was more significant than that of 5 mg/l Nim and 10 or 20 mg/l LBP.

Measurement of MMP

Differences in $\Delta\psi m$ were assessed using JC-1. Staining with JC-1 allows cells to be excited at two different wavelengths in order to assess $\Delta\psi m$ in cells undergoing oxidative stress or
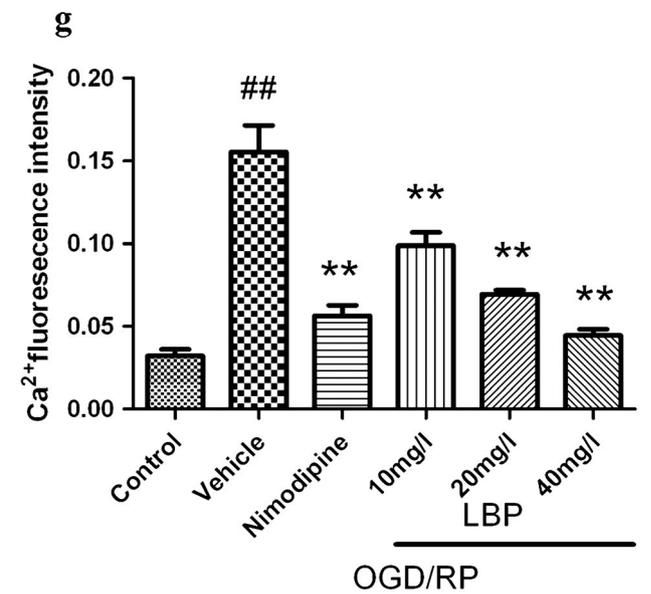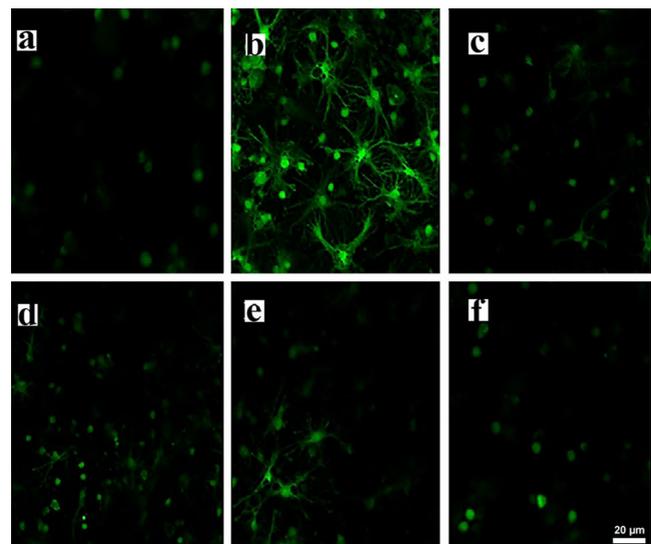

Fig. 2 Effects of LBP on $[Ca^{2+}]_i$ in primary hippocampal neuronal cells under OGD 2 h/RP 24 h as indicated by Fluo-3/AM (×200). **a** Control group; **b** Vehicle group; **c** Nim (5 mg/L) group; **d–f** LBP (10, 20, 40 mg/L) treatment groups; **g** effects of LBP on $[Ca^{2+}]_i$ in primary hippocampal neuronal cells under OGD 2 h/RP 24 h. *Histograms* represent mean $\pm$ SD, $n = 6$. $^{\#\#}p < 0.01$ *Vehicle* group vs. *Control* group; $^{*}p < 0.05$, $^{**}p < 0.01$ vs. *Vehicle* group

other challenges that would affect $\Delta\psi m$ such as apoptosis. Red fluorescence indicates polarized mitochondrial membranes whereas green fluorescence indicates depolarized mitochondrial membranes. The hippocampus treated with LBP exhibited a marked difference in JC-1 staining compared with neurons that were solely exposed to OGD/RP (Fig. 3). Neurons that were subjected to a model of OGD/RP showed a significant decrease in JC-1 red/green fluorescence ratio (0.175 ± 0.022), indicating that the mitochondrial membranes of cells that were exposed to OGD are more depolarized compared to cells that were treated with LBP (10, 20,
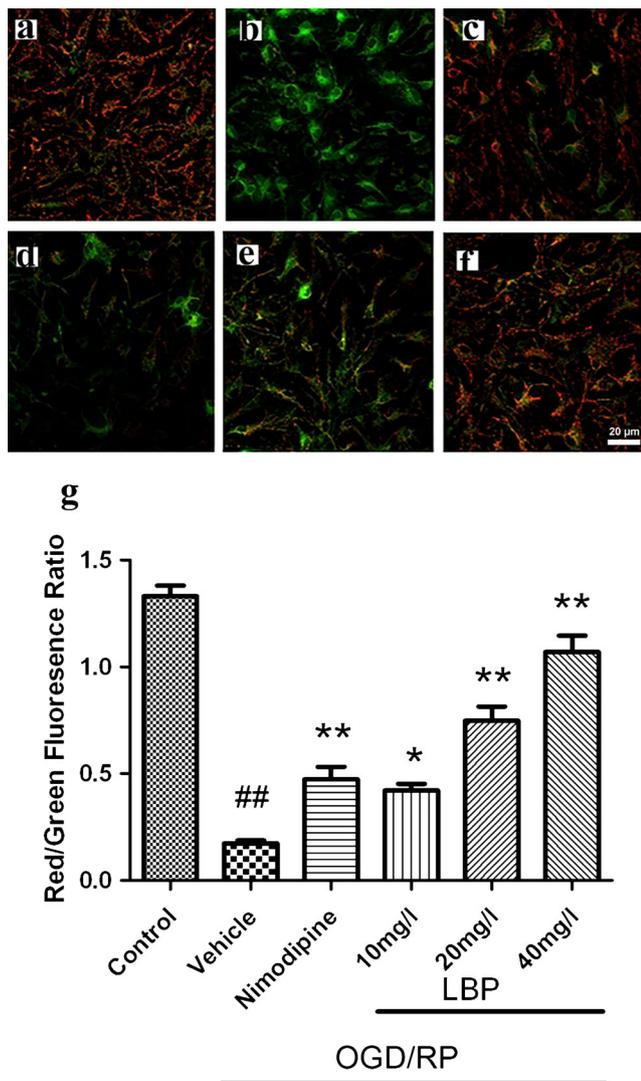
Fig. 3 Effects of LBP on MMP changes in primary hippocampal neuronal cells under OGD 2 h/RP 24 h as indicated by JC-1 (×200). **a** Control group; **b** Vehicle group; **c** Nim (5 mg/L) group; **d–f** LBP (10, 20, 40 mg/L) treatment groups; **g** effects of LBP on MMP in primary hippocampal neuronal cells under OGD 2 h/RP 24 h. *Histograms* represent mean ± SD, $n = 6$. $^{##}p < 0.01$ *Vehicle* group vs. *Control* group; $^{**}p < 0.01$ vs. *Vehicle* group

Fig. 4 Representative pictures of nuclei staining with Hoechst 33342 (×400). Representative photomicrographs showing the nuclear morphology of hippocampal neurons in Control (**a**), Vehicle (**b**), Nim (5 mg/L) treatment (**c**) and LBP (10, 20, 40 mg/L) treatment (**d–f**) groups. The percentage of nuclear condensation in the cultured neurons of different groups was counted (**g**). *Histograms* represent Mean ± SD, $n = 6$. $^{##}p < 0.01$ *Vehicle* group vs. *Control* group; $^{*}p < 0.05$, $^{**}p < 0.01$ vs. *Vehicle* group

40 mg/l) as compared to neurons incubated under normoxic conditions (1.33 ± 0.085, $P < 0.01$).

Protective effects of LBP pretreatment on OGD/RP induced apoptosis in cells

Hoechst 33342 staining (Fig. 4) showed that, in response to the OGD/RP insult, approximately 78% of cells displayed typical morphological features of apoptosis including chromatin condensation, nuclear shrinkage and the formation of a few apoptotic bodies. Pretreatment with 10, 20 and 40 mg/l LBP reduced the percentage of apoptotic cells by approximately 21, 43 and 65%, respectively.
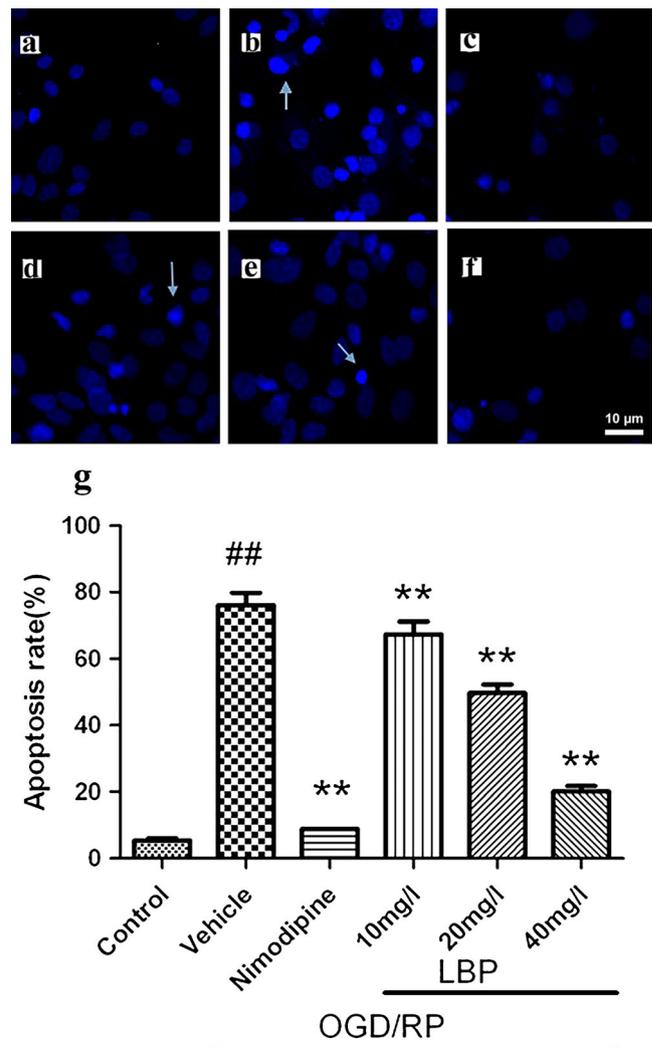
Neuronal viability and apoptosis were also assessed using the TUNEL assay. Figure 5 shows TUNEL-positive cells after untreatment of cells with LBP, whereas large numbers of TUNEL-positive cells were seen in the OGD/RP. In contrast, numbers of TUNEL-positive (green) cells in control groups were less. Quantitative analysis showed that the LBP (10, 20, 40 mg/l) pretreatment significantly reduced the number of TUNEL-positive cells; the cells were decreased in a dose-dependent manner, compared to the vehicle group.

LBP pretreatment affects OGD/RP induced expression of genes and proteins in cells NF-κB, TLR4, IL-6 and IκB-α. Those genes expressions were determined by measuring the messenger RNA levels using reverse transcription polymerase
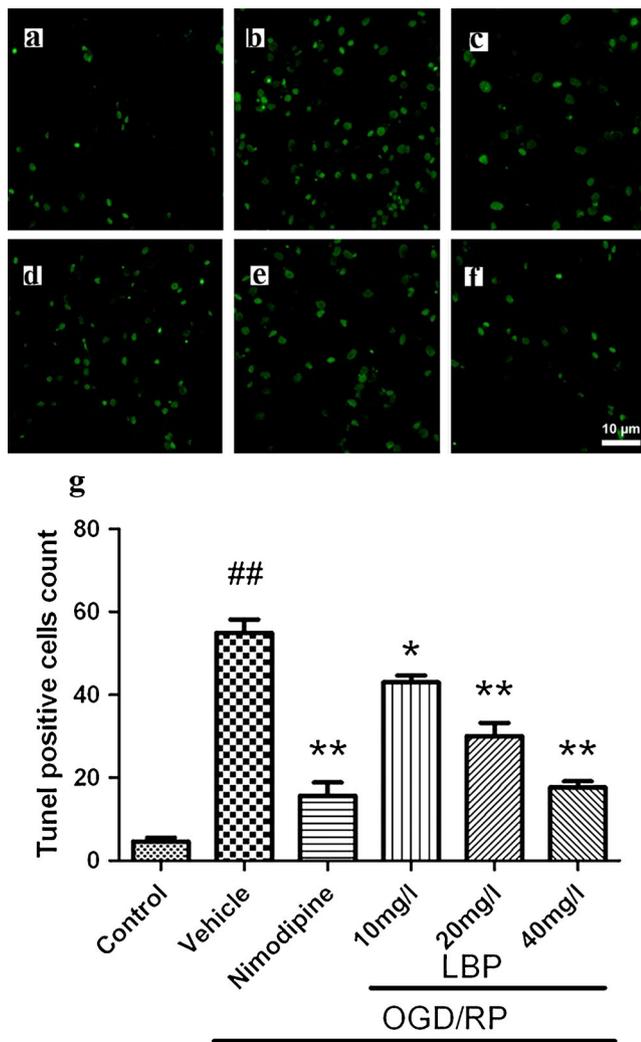
Fig. 5 LBP reduces the number of Tunel positive neurons after OGD/RP injury. Representative photomicrographs showing the nuclear morphology of hippocampal neurons in Control (**a**), Vehicle (**b**), Nim (5 mg/L) treatment (**c**) and LBP (10, 20, 40 mg/L) treatment (**d–f**) groups. The percentage of nuclear condensation in the cultured neurons of different groups was counted (**g**). Histograms represent Mean ± SD, $n = 6$. [##]$p < 0.01$ *Vehicle* group vs. *Control* group; [*]$p < 0.05$, [**]$p < 0.01$ vs. *Vehicle* group

chain reaction (RT-PCR). Increasing expression of IL-6, TLR4 and NF-κB ($P < 0.01$ compared to the vehicle group, Fig. 6a-c) and decreasing level of IκB-α were observed in OGD/RP ($P < 0.01$ compared to the vehicle group, Fig. 6d). LBP pretreatment significantly suppressed the OGD/RP induced increase in the IL-6, TLR4 and NF-κB mRNA levels ($P < 0.01$, $P < 0.05$ and $P < 0.05$, Fig. 6a-c) and increased the level of IκB-α ($P < 0.05$, Fig. 6d).

To further examine the signaling pathways involved in the neuroprotective effect of LBP against the OGD/RP insult in cells, the expressions of NF-κB, IκB-α, IL-6 and TLR4 were assessed by western blotting. As shown in Figs. 7 and 8, OGD/RP significantly increased the protein level IL-6, TLR4 and NF-κB ($P < 0.01$; Figs. 7a–c, 8a, b), while

decreasing the level of IκB-α ($P < 0.01$; Fig. 8a, c). However, 40 mg/l LBP treatment caused a significant decrease in NF-κB, IL-6 and TLR4 ($P < 0.05$; Fig. 7a–c; $P < 0.01$; Fig. 8a, b) and an increase in IκB-α expression compared with vehicle group ($P < 0.05$; Fig. 8a, c).

Discussion

Recent studies in the area of stroke and brain ischemia have demonstrated the significance of the inflammatory response, which contributes to ischemic pathology and anti-inflammatory strategies have become popular. The present study indicated that LBP regulates OGD/RP injury via the TLR4/NF-κB signaling way and this may be associated with oxidants.

We used a model of OGD/RP in the hippocampus as a way of reproducing clinical situations, since reperfusion can occur spontaneously through resolution of an embolus or clinical intervention and for evaluating the neuroprotective effect of LBP against the effect of detrimental reperfusion injury.

The study evaluated the degree of injury in hippocampal neuronal cells exposed to OGD/RP by MTT and LDH release. Treatment with LBP (10, 20, 40 mg/l) decreased cell damage and inhibited LDH release, which indicated that LBP may have a protective effect on hippocampal neuronal cells exposed to OGD/RP.

The protective effect of LBP was also supported by lower MMP. MMP reflects the performance of the electron transport chain and indicates a pathological disorder of this system. High average MMP is related to higher viability (Li et al. 2016). Our data indicated tht MMP levels decreased after 24 h reperfusion and treatment with LBP (10–40 mg/l) prevented the loss of MMP.

Abnormalities of $[Ca^{2+}]_i$ homeostasis, especially $[Ca^{2+}]_i$ overload, have been linked to neuronal apoptosis induced by ischemia–reperfusion (Su et al. 2016). Our results showed that OGD/RP insult caused an elevated $[Ca^{2+}]_i$ in the subjected neurons and pre-treatment with LBP inhibited cell apoptosis concentration-dependently, which was consistent with its anti-early apoptosis effect in the same model. The results suggested that the effect of LBP on neuronal apoptosis was, at least partly, involved in its depressing activity in the abnormal elevated $[Ca^{2+}]_i$ of the hippocampus.

Apoptosis plays a significant role in the pathophysiology of cerebral ischemia reperfusion injury (Chumboatong et al. 2017; Wu et al. 2016). Our previous researches demonstrated LBP improves cell survival in the OGD/RP. We further studied the anti-apoptotic effect on the same model by Hoechst 33342 and TUNEL staining. We found that the OGD/RP insult caused a remarkable increase in the neuronal apoptotic percentage, which was depressed by the administration of LBP in a concentration-dependent manner and elicited an
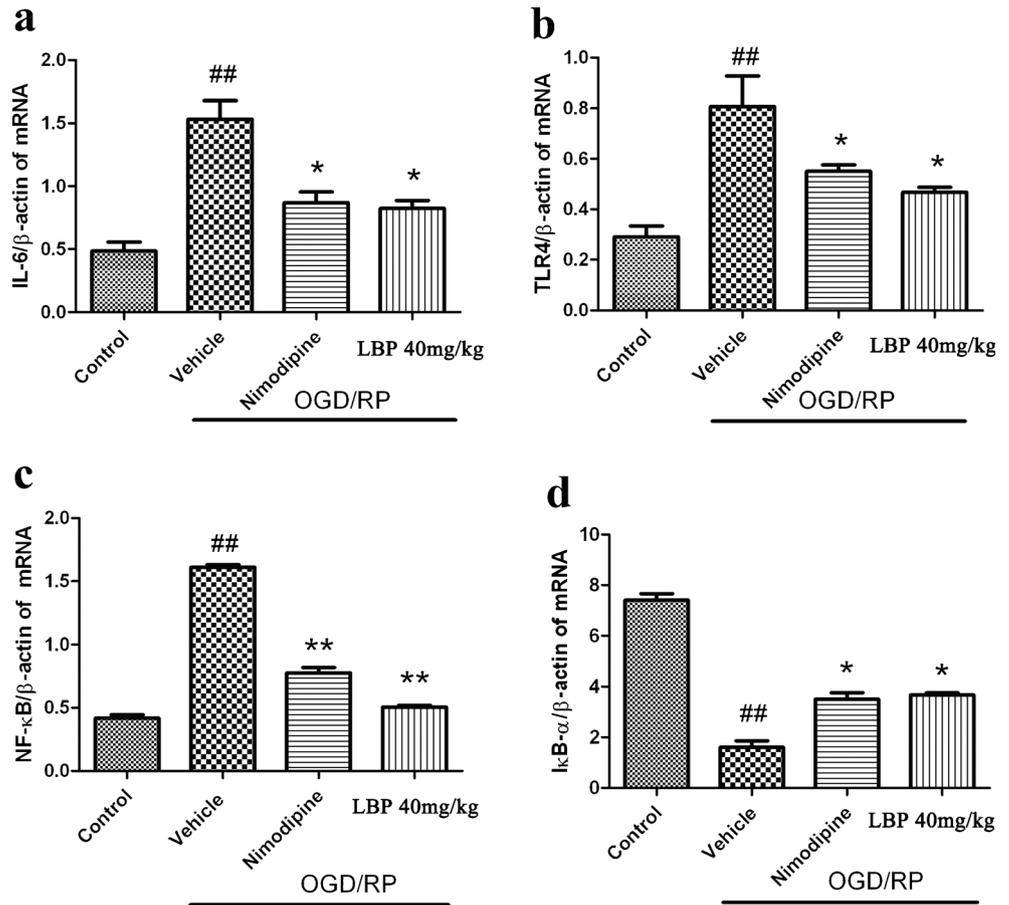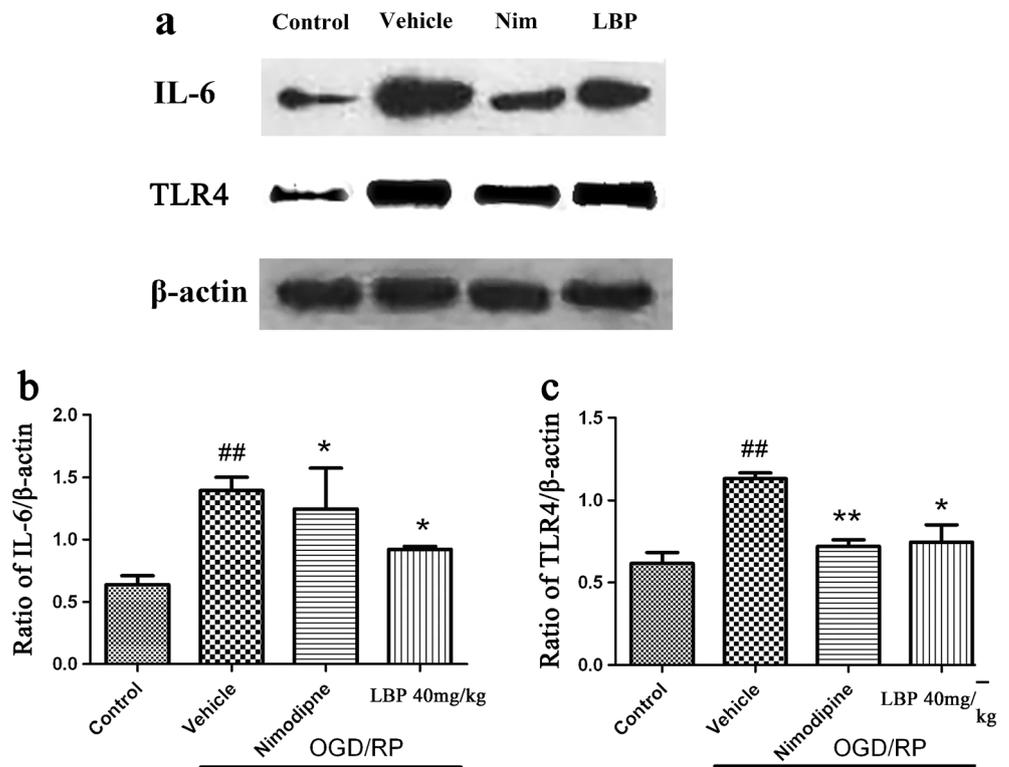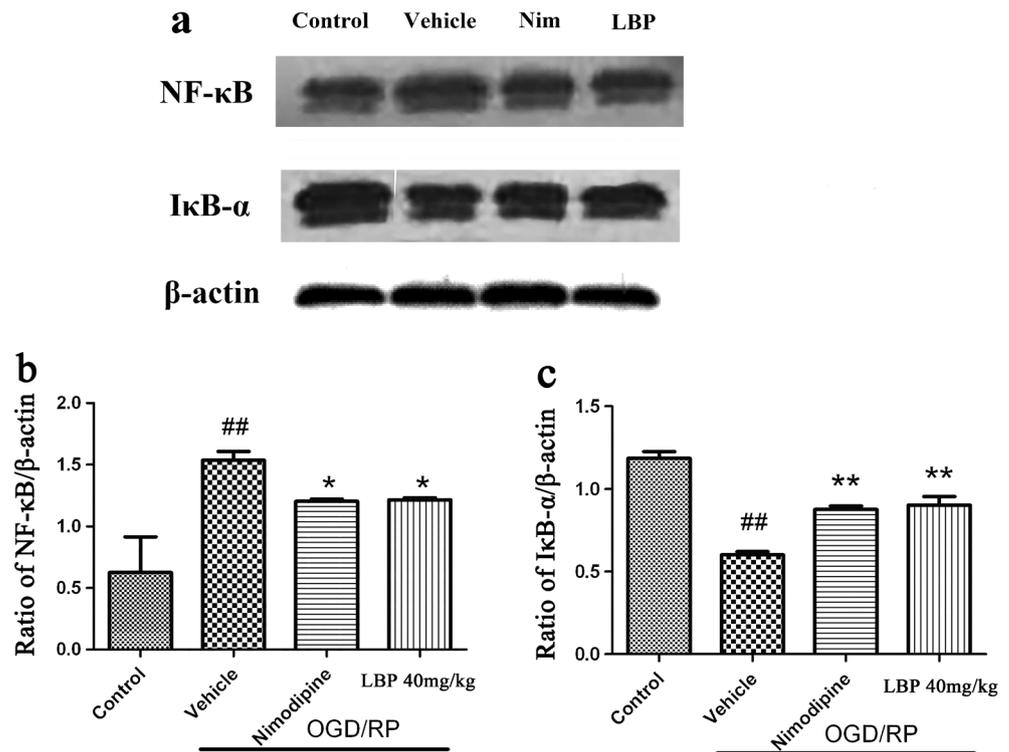
Fig. 8 Effect of LBP on the expression of NF-κB and IκB-α (**a**) protein expression in the hippocampal neurons as determined by western blot. Densitometric analyses of western blot presented as mean ± SD, $n = 6$ and the data are presented as the fold induction over control cells (**b**, **c**). $^{\#\#}p < 0.01$ *Vehicle* group vs. *Control* group; $^{*}p < 0.05$, $^{**}p < 0.01$ vs. *Vehicle* group

obvious abnormal neuronal morphological change. All these facts demonstrated that the anti-apoptotic activity of LBP contributed to the beneficial effect on neuronal injury in this model.

OGD/RP enhances the formation of ROS in brain tissue. ROS is directly involved in oxidative cellular damage, leading to cell death (Willcox and Summerlee 2014). Cells that are experiencing oxidative stress produce an imbalance of ROS that overwhelms the endogenous ROS scavenging systems and further oxidative damage resulting in the disruption of cellular proteins, lipids, polysaccharides and DNA (Valero 2014; Maciejczyk et al. 2016; Ji et al. 2007; Nagayama et al. 2000). We observed substantial decreases in ROS generation and apoptosis in rat hippocampus cultures at doses of 10, 20 and 40 mg/l LBP when compared to cells that were exposed to OGD/RP alone.

ROS can then stimulate ischemic cells, even ischemic neurons, to secrete inflammatory cytokines and chemokines (Bonaventura et al. 2016). Inflammation induced by oxidant stress has many of the features associated with classical activation of the innate immune system and, as such, resemble that seen after activation of TLRs (Karki and Igwe 2013; Deng et al. 2016). Both TLR2 and TLR4 function in the MyD88-dependent pathway to activate NF-κB, which induces the expression of proinflammatory genes, inflammatory cytokines and adhesion molecules and the activation of adaptive immunity (Gu et al. 2012; Wang et al. 2016; Winters et al. 2013). TLR4 was also found to be more important than other TLRs in the pathologic progression of cerebral ischemia and reperfusion. It mediates pro-inflammatory responses through NF-κB

and other sensors, which induce the upregulation of pro-inflammatory factors (Eltzschig and Eckle 2011; Ma et al. 2013). Our results showed that OGD/RP induced an increase of the mRNA and protein expression of TLR4. Treatment with LBP showed an obvious suppression.

It has been shown that continuously active TLR4 can induce the activation of NF-κB with consequent expression of a number of proinflammatory cytokines and a co-stimulatory molecule (Han et al. 2017). NF-κB is a central mediator of the inflammatory processes that exist in an inactive form by associating with an inhibitory protein of the IκB family, which is a family of proteins consisting of IκB-α, IκB-β and IκB-γ, which can inhibit the activation of the NF-κB transcription factor. In unstimulated cells, NF-κB resides in the cytoplasm as a complex with inhibitory IκB proteins that mask their nuclear localization signal. Upon cell activation, IκB is phosphorylated and proteolytically degraded, resulting in the translocation of NF-κB to the nucleus (Ma et al. 2013; Yuan et al. 2013) causing cell death. In this study, LBP (40 mg/l) significantly reduced the protein levels of NF-κB and inhibited the OGD/RP-induced degradation of IκB-α. Therefore, our data strongly support the theory that TLR4 is implicated in LBP neuroprotection after cerebral ischemia through the inhibition of NF-κB activation.

Similarly, other experiments revealed that TLR4 could regulate the expression of cytokines, such as TNF-α, COX-2, IL-6 and iNOS (Tu et al. 2010; Zhou et al. 2016a, b; Wang et al. 2015a, b). IL-6 possesses multiple biological functions and a variety of cytokines can induce the production of IL-6, which

can be detected in brain tissue, cerebrospinal fluid and serumat reperfusion 2 h after cerebral ischemia. Some studies have shown that IL-6 can stimulate generated neurotrophic factors and nervous growth factors, which assist the repair of damaged nervous cells but also participate in the inflammatory injuries (Gertz et al. 2012). In this study, LBP (40 mg/l) was administered 24 h after reperfusion in an ischemic model. Our data in neuronal cultures confirmed that LBP(40 mg/l) ameliorated the IL-6 expression.

Taken together, we have provided evidence that LBP exhibited anti-oxidant and anti-inflammatory activities capable of regulating TLR4/NF-κB signaling in vitro. Therefore, LBP may be used as an effective neuroprotective agent for the treatment of stroke in clinical trials and holds promise for the development of new therapeutic approaches. It is worth noting that a weakness of the finding is that we did not have information for the effects of LBP in non-OGD condition. Future study will test whether LBP rescues levels of pro-inflammatory molecules at the baseline or if this is specific to OGD-induced injury.

In conclusion, our data show that LBP regulated OGD/RP injury via the TLR4/NF-κB signaling way and this may be associated with oxidants. A better understanding of the mechanisms that underlie the hippocampal response during the course of OGD/RP will be useful in improving treatment of brain ischemia.

Compliance with ethical standards

Competing interests The authors declare that they have no competing interests.

References

Bonaventura A, Liberale L, Vecchié A, Casula M, Carbone F, Dallegri F, Montecucco F (2016) Update on Inflammatory Biomarkers and Treatments in Ischemic Stroke. Int J Mol Sci 17(12)

Burke JF, Lisabeth LD, Brown DL, Reeves MJ, Morgenstern LB (2012) Determining stroke's rank as a cause of death using multicause mortality data. Stroke 43:2207–2211. doi:10.1161/STROKEAHA.112.656967

Chang RC, So KF (2008) Use of anti-aging herbal medicine, *Lycium barbarum*, against aging-associated diseases. What do we know so far? Cell Mol Neurobiol 28:643–652

Chumboatong W, Thummayot S, Govitrapong P, Tocharus C, Jittiwat J, Tocharus J (2017) Neuroprotection of agomelatine against cerebral ischemia/reperfusion injury through an antiapoptotic pathway in rat. Neurochem Int 102:114–122. doi:10.1016/j.neuint.2016.12.011

Deng L, Pan J, Peng Q, Dong Z, Wang Y (2016) Toll-like receptor 3 and interferon β mRNA expressions were increased in peripheral blood of ischemic stroke patients with good outcome. J Stroke Cerebrovasc Dis. doi:10.1016/j.jstrokecerebrovasdis.2016.11.122

Eltzschig HK, Eckle T (2011) Ischemia and reperfusion–from mechanism to translation. Nat Med 17:1391-401. doi:10.1038/nm.2507

Gertz K, Kronenberg G, Kälin RE, Baldinger T, Werner C, Balkaya M, Eom GD, Hellmann-Regen J, Kröber J, Miller KR, Lindauer U, Laufs U, Dirnagl U, Heppner FL, Endres M (2012) Essential role of interleukin-6 in post-stroke angiogenesis. Brain 135:1964–1980. doi:10.1093/brain/aws075

Gu JH, Ge JB, Li M, Wu F, Zhang W, Qin ZH (2012) Inhibition of NF-kB activation is associated with anti-inflammatory and anti-apoptotic effects of Ginkgolide B in a mouse model of cerebral ischemia/reperfusion injury. Eur J Pharm Sci 47:652–660. doi:10.1016/j.ejps.2012.07.016

Gwag BJ, Lobner D, Koh JY, Wie MB, Choi DW (1995) Blochade of glutamate receptors unmasks neuronal apoptosis after oxygen-glucose deprivation in vitro. Neuroscience 68:615–619

Han J, Zou C, Mei L, Zhang Y, Qian Y, You S, Pan Y, Xu Z, Bai B, Huang W, Liang G (2017) MD2 mediates angiotensin II-induced cardiac inflammation and remodeling via directly binding to Ang II and activating TLR4/NF-κB signaling pathway. Basic Res Cardiol 112:9. doi:10.1007/s00395-016-0599-5

He M, Pan H, Chang RC, So KF, Brecha NC, Pu M (2014) Activation of the Nrf2/HO-1 antioxidant pathway contributes to the protective effects of *Lycium barbarum* polysaccharides in the rodent retina after ischemia-reperfusion-induced damage. PLoS ONE 9:e84800. doi:10.1371/journal.pone.0084800 eCollection 2014

Huyan T, Li Q, Yang H, Jin M-L, Zhang M-J, Ye L-J, Li J, Huang Q-S, Yin D-C (2014) Protective effect of polysaccharides on simulated microgravity-induced functional inhibition of human NK cells. Carbohydr Polym 101:819–827. doi:10.1016/j.carbpol.2013.10.021

Ji X, Luo Y, Ling F, Stetler RA, Lan J, Cao G, Chen J (2007) Mild hypothermia diminishes oxidative DNA damage and pro-death signaling events after cerebral ischemia: a mechanism for neuroprotection. Front Biosci 12:1737–1747

Kaczorowski DJ, Mollen KP, Edmonds R, Billiar TR (2008) Early events in the recognition of danger signals after tissue injury. J Leukoc Biol 83:546–552

Karki R, Igwe OJ (2013) Toll-like receptor 4–mediated nuclear factor kappa B activation is essential for sensing exogenous oxidants to propagate and maintain oxidative/Nitrosative cellular stress. PLoS ONE 8(9):e73840. doi:10.1371/journal.pone.0073840 eCollection 2013

Krmpotić L, Zirdum D, Gorup D et al (2013) Expression analysis of genes involved in TLR2-related signaling pathway: inflammation and apoptosis after ischemic brain injury. Neuroscience 238:87–96

Li Y, Wang M, Wang S (2016) Effect of inhibiting mitochondrial fission on energy metabolism in rat hippocampal neurons during ischemia/reperfusion injury. Neurol Res 14:1–8

Livak KJ, Schmittgen TD (2001) Analysis of relative gene expression data using real-time quantitative PCR and the 2(−Delta Delta C(T)) method. Methods 25:402–408

Ma Y, He M, Qiang L (2013) Exercise therapy down regulates the overexpression of TLR4, TLR2, MyD88 and NF-κB after cerebral ischemia in rats. Int J Mol Sci 14:3718–3733. doi:10.3390/ijms14023718

Maciejczyk M, Mikoluc B, Pietrucha B, Heropolitanska-Pliszka E, Pac M, Motkowski R, Car H (2016) Oxidative stress, mitochondrial abnormalities and antioxidant defense in ataxia-telangiectasia. Bloom Syndr Nijmegen Breakage Syndr 11:375–383. doi:10.1016/j.redox.2016.12.030

Nagayama T, Lan J, Henshall DC, Chen D, O'Horo C, Simon RP, Chen J (2000) Induction of oxidative DNA damage in the peri-infarct region after permanent focal cerebral ischemia. J Neurochem 75:1716–1728

Reers M, Smith TW, Chen LB (1991) J-aggregate formation of a carbocyanine as a quantitative fluorescent indicator of membrane potential. Biochemistry 30:4480–4486

Rui C, Yuxiang L, Yinju H, Qingluan Z, Yang W, Qipeng Z, Hao W, Lin M, Juan L, Chengjun Z, Yuanxu J, Yanrong W, Xiuying D, Wannian Z, Tao S, Jianqiang Y (2012) Protective effects of *Lycium barbarum* polysaccharide on neonatal rat primary cultured hippocampal neurons injured by oxygen-glucose deprivation and reperfusion. J Mol Histol 43:535–542. doi:10.1007/s10735-012-9420-4

Strong K, Mathers C, Bonita R (2007) Preventing stroke: saving lives around the world. Lancet Neurol 6:182–187

Su F, Guo AC, Li WW, Zhao YL, Qu ZY, Wang YJ, Wang Q, Zhu YL (2016) Low-Dose Ethanol Preconditioning Protects Against Oxygen-Glucose Deprivation/Reoxygenation-Induced Neuronal Injury By Activating Large Conductance, Ca^{2+}-Activated K^+ Channels In Vitro. Neurosci Bull

Tu XK, Yang WZ, Shi SS, Wang CH, Zhang GL, Ni TR, Chen CM, Wang R, Jia JW, Song QM (2010) Spatio-temporal distribution of inflammatory reaction and expression of TLR2/4 signaling pathway in rat brain following permanent focal cerebral ischemia. Neurochem Res 35:1147–1155. doi:10.1007/s11064-010-0167-6

Valero T (2014) Mitochondrial biogenesis: pharmacological approaches. Curr Pharm Des 20:5507–5509

Varoni MV, Pasciu V, Gadau SD, Baralla E, Serra E, Palomba D, Demontis MP (2016) Possible antioxidant effect of *Lycium barbarum* polysaccharides on hepatic cadmium-induced oxidative stress in rats. Environ Sci Pollut Res Int

Wang T, Li Y, Wang Y, Zhou R, Ma L, Hao Y, Jin S, Du J, Zhao C, Sun T, Yu J (2014) *Lycium barbarum* Polysaccharide prevents focal cerebral ischemic injury by inhibiting neuronal apoptosis in mice. PLoS ONE 9:e90780. doi:10.1371/journal.pone.0090780 eCollection 2014

Wang H, Lau BW, Wang NL, Wang SY, Lu QJ, Chang RC, So KF (2015a) *Lycium barbarum* polysaccharides promotes in vivo proliferation of adult rat retinal progenitor cells. Neural Regen Res 10(12): 1976–1981. doi:10.4103/1673-5374.172315

Wang PF, Xiong XY, Chen J, Wang YC, Duan W, Yang QW (2015b) Function and mechanism of toll-like receptors in cerebral ischemic tolerance: from preconditioning to treatment. J Neuroinflammation 12:80. doi:10.1186/s12974-015-0301-0

Wang Y, Chen G, Yu X, Li Y, Zhang L, He Z, Zhang N, Yang X, Zhao Y, Li N, Qiu H (2016) Salvianolic acid B ameliorates cerebral ischemia/reperfusion injury through inhibiting TLR4/MyD88 signaling pathway. Inflammation 39:1503–1513. doi:10.1007/s10753-016-0384-5

Willcox JM, Summerlee AJ (2014) Relaxin protects astrocytes from hypoxia in vitro. PLoS ONE 9:e90864. doi:10.1371/journal.pone.0090864 eCollection 2014

Winters L, Winters T, Gorup D, Mitrečić D, Curlin M, Križ J, Gajović S (2013) Expression analysis of genes involved in TLR2-related signaling pathway: inflammation and apoptosis after ischemic brain injury. Neuroscience 238:87–96. doi:10.1016/j.neuroscience.2013.02.001

Wu GJ, Chen JT, Tsai HC, Chen TL, Liu SH, Chen RM (2016) Protection of dexmedetomidine against ischemia/reperfusion-induced apoptotic insults to neuronal cells occurs via an intrinsic mitochondria-dependent pathway. J Cell Biochem. doi:10.1002/jcb.25847

Xiao J, Xing F, Huo J, Fung ML, Liong EC, Ching YP, Xu A, Chang RC, So KF, Tipoe GL (2014) *Lycium barbarum* polysaccharides therapeutically improve hepatic functions in non-alcoholic steatohepatitis rats and cellular steatosis model. Sci Rep 4:5587. doi:10.1038/srep05587

Yuan S, Zhang J, Zhang L, Huang L, Peng J, Huang S, Chen S, Xu A (2013) The archaic roles of the amphioxus NF-κB/IκB complex in innate immune responses. J Immunol 19:1220–1230. doi:10.4049/jimmunol.1203527

Zhang M, Chen H, Huang J, Li Z, Zhu C, Zhang S (2005) Effect of *Lycium barbarum* polysaccharide on human hepatoma QGY7703 cells: inhibition of proliferation and induction of apoptosis. Life Sci 76:2115–2124

Zhang XJ, Yu HY, Cai YJ, Ke M (2016) *Lycium barbarum* polysaccharides inhibit proliferation and migration of bladder cancer cell lines BIU87 by suppressing Pi3K/AKT pathway. Oncotarget. doi:10.18632/oncotarget.13963

Zhao J, Liu R (2016) Stroke 1-2-0: a rapid response programme for stroke in China. Lancet Neurol. doi:10.1016/S1474-4422(16)30283-6

Zhao J, Wu Y, Sun M, Wang J, Li YH, Zhang K, Yu JQ (2012) Protective effects and mechanisms of OSR on primary cultured hippocampus neurons subjected to anoxic injury in neonatal rat. Chin J Chin Mater Med 37:94–98

Zhao R, Qiu B, Li Q, Zhang T, Zhao H, Chen Z, Cai Y, Ruan H, Ge W, Zheng X (2014) LBP-4a improves insulin resistance via translocation and activation of GLUT4 in OLETF rats. Food Funct 5:811–820. doi:10.1039/c3fo60602c

Zhou JM, Gu SS, Mei WH, Zhou J, Wang ZZ, Xiao W (2016a) Ginkgolides and bilobalide protect BV2 microglia cells against OGD/reoxygenation injury by inhibiting TLR2/4 signaling pathways. Cell Stress Chaperones 21:1037–1053

Zhou J, Pang H, Li W, Liu Q, Xu L, Liu Q, Liu Y (2016b) Effects of *Lycium barbarum* polysaccharides on apoptosis, cellular adhesion, and oxidative damage in bone marrow mononuclear cells of mice exposed to ionizing radiation injury. Biomed Res Int 2016:4147879. doi:10.1155/2016/4147879

Zhu XJ, Shi Y, Peng J, Guo CS, Shan NN, Qin P, Ji XB, Hou M (2009) The effects of BAFF and BAFF-R-Fc fusion protein in immune thrombocytopenia. Blood 114:5362–5367. doi:10.1182/blood-2009-05-217513